ChemPubSoc Europe

DOI: 10.1002/cctc.201200520

Palladium-Catalyzed Ethylene/Methyl Acrylate Cooligomerization: Effect of a New Nonsymmetric α-Diimine

Angelo Meduri,[a] Tiziano Montini,[a] Fabio Ragaini,[b] Paolo Fornasiero,[a] Ennio Zangrando,[a] and Barbara Milani*[a]

A new nonsymmetric bis(aryl-imino)acenaphthene (Ar-BIAN) ligand, featured by a subtle steric and electronic unbalance of the N-donor atoms, is reported. With the new ligand and the corresponding symmetrically substituted derivatives, both neutral and monocationic Pd–CH_3 compounds have been synthesized and characterized. The series of the monocationic complexes $[Pd(CH_3)(L)(Ar\text{-}BIAN)][PF_6]$ (L = CH_3CN, dmso) has been extended to dimethyl sulfoxide derivatives. The monocationic complexes are tested as precatalysts for the ethylene/methyl acrylate cooligomerization under mild reaction conditions of temperature and ethylene pressure. The catalytic product is a mixture of ethylene/acrylate cooligomers and higher alkenes. The catalysts containing the new nonsymmetric ligand are found to be more productive than those with the symmetric Ar-BIANs. The Pd–dmso catalysts are more productive and show a longer lifetime than their Pd–$NCCH_3$ counterparts.

Introduction

Functionalized polymers featured by a polyolefin skeleton modified with polar groups represent highly desirable materials that should express surface properties, such as adhesion, dye-ability, printability, and compatibility, that are insufficiently present in unmodified polyolefins.[1–6] Commercial processes for the incorporation of polar monomers are currently based either on radical polymerization or on post-polymerization functionalization—two technologies that suffer from high energy consumption, low cost-efficiency, and poor control over the polymer microstructure. To overcome these problems, the most straightforward approach used is based on the development of highly efficient catalysts for the controlled, direct copolymerization of terminal alkenes with polar monomers. The discovery of such a catalyst has been indicated as one of the "holy grails" in the field of olefin polymerization.[7]

Although the use of early transition metals, applied usually as catalysts for polyolefin synthesis, is hampered because of their oxophilicity, Brookhart's discovery that compounds based on late transition metals are efficient catalysts for ethylene polymerization[8,9] opens the way to apply them in the ethylene/polar monomer copolymerization. The two main catalytic systems reported in the literature are based on palladium complexes and differ in the nature of the ancillary ligand present in the metal coordination sphere, which in one case is a neutral α-diimine[10,11] and in the other an anionic phosphine sulfonate derivative (P–O) (Figure 1).[12]

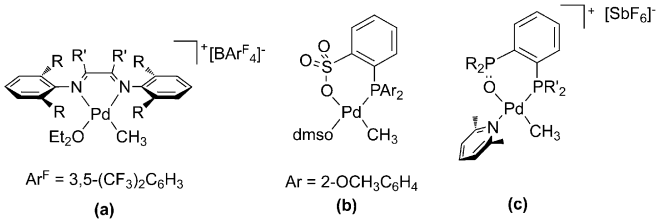

Figure 1. The three classes of complexes reported in the literature: a) α-diimino derivatives; b) phosphine sulfonate derivative; c) bisphosphine monoxide derivatives.

In the copolymerization of ethylene with methyl acrylate (MA), the model reaction, both catalytic systems lead to real copolymers and not to a mixture of two homopolymers. The two catalytic systems are operative under quite different reaction conditions that limit a direct comparison of the catalytic results. Nevertheless, some differences are evident: the α-diimine system leads to amorphous copolymers with a number average molecular weight of 300–88 000, with an incorporation of the polar monomer content from 1.0 to 12.1% into the branches of the polymer chain;[10] the P–O system leads to the copolymer with a number average molecular weight of 3900–12 800, with an incorporation of the polar monomer content from 3 to 17% into the linear polyethylene backbone.[12] In the case of the P–O system, a remarkable improvement in the catalytic performances is realized moving from the in situ catalytic system to preformed complexes;[13] for example, $[Pd(CH_3)$-

[a] A. Meduri, Dr. T. Montini, Prof. Dr. P. Fornasiero, Prof. E. Zangrando, Dr. B. Milani
Department of Chemical and Pharmaceutical Sciences
University of Trieste, Via Licio Giorgieri 1, 34127 Trieste (Italy)
Fax: (+39) 0405583903
E-mail: milaniba@units.it

[b] Prof. Dr. F. Ragaini
Department of Chemistry
University of Milano, Via C. Golgi 19, 20133 Milano (Italy)

Supporting information for this article contains crystal data, details of the structure solution, and refinements, NMR spectra of complexes and ethylene/MA cooligomers, in situ reactivity investigations, GC–MS analyses and their Poisson fitting, and modeling of the oligomer growth rate, and is available on the WWW under http://dx.doi.org/10.1002/cctc.201200520.

(dmso)(P–O)] yields the copolymer with a content of MA up to 52%.[14]

In addition, the catalysts based on the P–O system are quite versatile because they can catalyze the copolymerization of ethylene with various polar monomers, such as vinyl acetate,[15] acrylonitrile,[16] allyl monomers,[17] alkyl vinyl ether,[18] and vinyl fluoride.[19] They were also used for emulsion copolymerization[20] and for the copolymerization of ethylene with nitrogen-containing polar monomers.[21]

Contrarily, the literature on the α-diimine system is rather limited and the system has been extended to a peculiar cyclophane-modified ligand[22] that yields an ethylene/MA copolymer containing 21.8% of the polar monomer. The Pd–α-diimine system also catalyzes the copolymerization of 1-hexene with silyl vinyl ether[23] and of ethylene with 2-hydroxyethyl acrylate.[24]

A palladium catalytic system with a bisphosphine monoxide ligand catalyzes the copolymerization of ethylene with many polar monomers but MA, which leads to the highly linear copolymers with a random distribution of the polar functional groups into the polymer chain (Figure 1c).[25]

For these catalytic systems, the productivity is not practical and the discovery of highly efficient and inexpensive catalysts is a crucial challenge.[7]

We studied a series of α-diimine ligands featured by the acenaphthene skeleton and the aryl rings substituted in the *meta* position (^{m}Ar-BIAN).[26] The corresponding palladium complexes, [Pd(CH_3)($NCCH_3$)(^{m}Ar-BIAN)][PF_6], are efficient catalysts for the CO/vinyl arene copolymerization, which leads to polyketones with an atactic microstructure. The precatalysts with the nonsymmetrically substituted ^{m}Ar-BIAN were found to be more productive than those with the related symmetrically substituted ligands, which thus indicates that the unbalance of the electronic properties of the ligand has a positive effect on the catalytic performances. On the basis of these considerations and with the aim of creating both a steric and an electronic unbalance of the two N-donor atoms, the series of nonsymmetric Ar-BIANs has been extended to a new compound featured by an aryl ring with an electron-withdrawing group on the *meta* positions and the other ring with an electron-releasing group on the *ortho* positions (**1**; Figure 2).

With ligand **1** and the corresponding symmetrically substituted derivatives **2** and **4**, two series of monocationic palladium compounds were synthesized: [Pd(CH_3)(L)(Ar-BIAN)][PF_6] (L = CH_3CN, dmso). Although the complexes with dimethyl sulfoxide have been investigated extensively with P–O ligands,[14,27,28] this is the first report in which Pd–dmso complexes are used in conjunction with α-diimine ligands. The catalytic behavior of these complexes in ethylene/MA cooligomerization has been investigated in detail along with mechanistic studies.

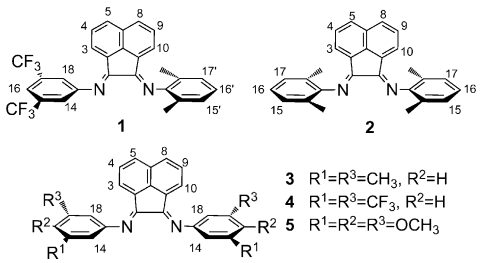

Figure 2. The studied α-diimines, **1**–**5**, and their numbering scheme.

The importance of having a nonsymmetric ligand on palladium for this catalysis has been highlighted by the catalytic behavior of palladium complexes with the P–O ligand. Here it is of interest to evaluate whether a subtle differentiation of the two N-donor atoms could result in remarkable effects on the catalytic performances.

Results and Discussion

Synthesis and characterization of ligand 1 and of its palladium complexes

Ligand **1** [(2,6-dimethyl-phenyl),(3,5-bis(trifluoromethyl)phenyl) diiminoacenaphthene] was synthesized by using a method slightly modified with respect to that reported previously for the nonsymmetrically substituted ^{m}Ar-BIANs.[26,29] In the transimination reaction, the zinc chlorido derivative coordinated with ligand **4** was reacted with 2,6-dimethyl aniline (Scheme 1) at room temperature for several days. The oil obtained after zinc decoordination contained ligand **1** together with the unreacted aniline and 3,5-bis(trifluoromethyl) aniline.

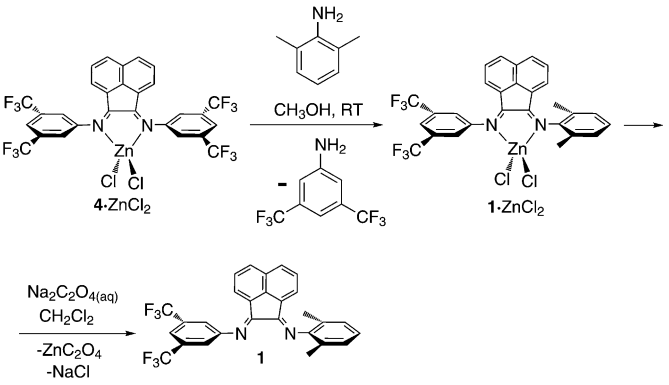

Scheme 1. Synthesis of ligand **1**.

Ligand **1** was isolated in good yield (up to 45%) from the crude reaction mixture by using column chromatography. As an alternative methodology, the crude oil can be reacted directly with [Pd(CH_3)Cl(cod)] (cod = 1,5-cyclooctadiene), which leads to pure [Pd(CH_3)Cl(**1**)] (**1a**).

In general, the synthesis of nonsymmetrically substituted Ar-BIANs is not so trivial. Several attempts to synthesize the sterically more hindered nonsymmetric ligand [(2,6-di-isopropyl-phenyl),(3,5-bis(trifluoromethyl)phenyl)] diiminoacenaphthene either through a transimination reaction or in two steps have failed. The mixtures of products were obtained, from which only the symmetric Ar-BIAN ligand with four isopropyl groups could be isolated in a pure form.

Ligand **1** was characterized both in the solid state and in solution. For BIAN ligands, (*E*,*E*) and (*E*,*Z*) isomers are possible depending on the relative configuration of the aryl rings with respect to C=N imine bonds.[30] For Ar-BIAN ligands, the (*E*,*E*) isomer is preferentially observed in the solid state,[30–34] except for few, such as the ligands featured by biphenyl or naphthyl substituents showing the (*E*,*Z*) isomer as the only molecule present in the unit cell.[35,36]

Suitable crystals for X-ray analysis of **1** were obtained by slow diffusion of hexane into a dichloromethane solution at 4 °C (Figure 3).

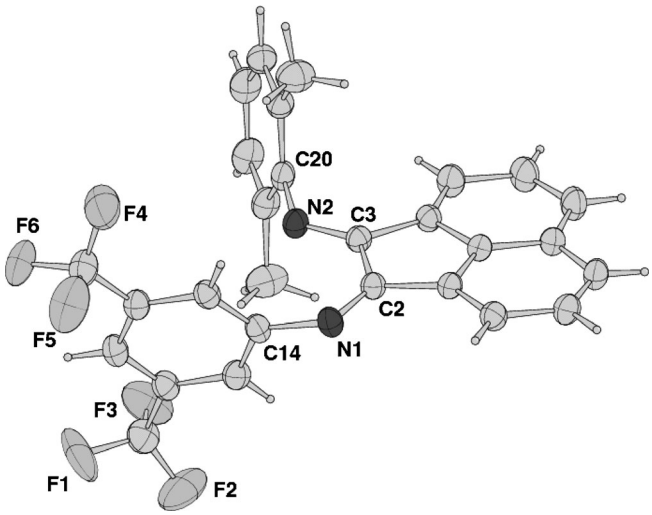

Figure 3. ORTEP drawing (thermal ellipsoids at the 30% probability level) of ligand **1**. Of the disordered F1-3 group, only flourines at higher occupancy are shown.

Ligand **1** shows a (*E*,*Z*) isomeric preference over the (*E*,*E*) pattern adopted on coordination. The different nature and position of substituents at imino units do not lead to important differences in bond lengths involving the imino nitrogens [N(1)–C(14) = 1.414(3), N(2)–C(20) = 1.426(3), N(1)–C(2) = 1.275(3), N(2)–C(3) = 1.277(3) Å], and these values are also maintained within their estimated standard deviations upon coordination in complex **1a**. The dihedral angle between the phenyl ring plane and the acenaphthene plane is 74.22(7)° for the (*Z*)-3,5-bis(trifluoromethyl)phenyl ring and 84.53(7)° for the (*E*)-2,6-dimethyl-phenyl ring.

The ^{1}H NMR spectrum, at room temperature, of a dichloromethane solution of **1** shows the signals of both (*E*,*E*) and (*E*,*Z*) isomers in equimolar ratio; the composition of the isomeric mixture varies with the solvent: (*E*,*E*)/(*E*,*Z*) = 2:1 in $CDCl_3$ solution. The two isomers are in equilibrium with slow rate on the NMR timescale, as usually observed for these molecules.[30,31]

Ligand **1** was reacted with [Pd(CH_3)Cl(cod)], which yielded the corresponding neutral complex **1a** (Scheme 2). The NMR characterization in CD_2Cl_2 solution reveals the presence of exclusively one species that, by a NOESY experiment, has been identified as the isomer with the Pd–CH_3 moiety *trans* to the Pd–N bond of the *meta*-substituted ring. For the sake of clarity, this species is designated as the *trans* isomer (Figure 4). Traces

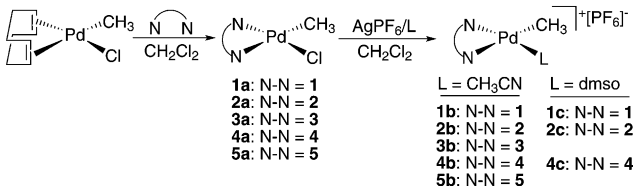

Scheme 2. Synthesis of palladium complexes **1a**–**5a**, **1b**–**5b**, **1c**, **2c**, and **4c**.

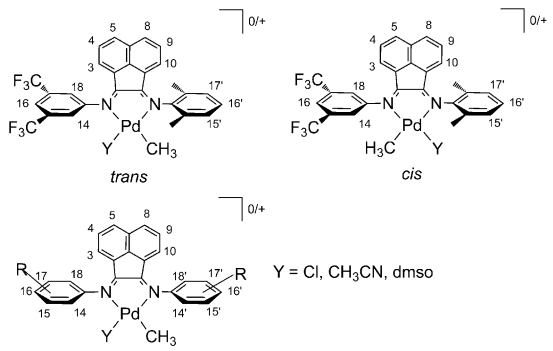

Figure 4. Schematic drawing of *cis* and *trans* isomers and of the complexes with the symmetric Ar-BIAN ligands. For R, see Figure 2.

of the *cis* isomer are observed. This is in agreement with the stronger *trans* influence of the methyl group with respect to chlorido and the weaker coordinating strength of the nitrogen atom bearing the trifluoromethyl-substituted aryl group with respect to that containing the methyl groups. The two isomers are in equilibrium as demonstrated by both NOESY and ROESY experiments.

In agreement with the NMR data of analogous Pd–(Ar-BIAN) complexes,[26,37] owing to coordination to palladium the signals of H^3 and H^{10} are shifted in the opposite direction with respect to the same signals in the free ligand, which is the doublet of H^3 at a frequency higher than that of H^{10}. This shift is attributed to its position *cis* to the chlorido ligand.[38] The singlet of Pd–CH_3 is sensitive to the nature of Ar-BIAN coordinated to the metal center: in complex **4a** it resonates at 0.78 ppm, in **1a** at 0.72 ppm, and in **2a** at 0.61 ppm, moving to shielding direction on increasing the electron density on the N-donor atoms and therefore on palladium.

Suitable crystals for complex **1a** were obtained by using a crystallization method based on slow diffusion of hexane into a chloroform solution of the complex at 4 °C. The crystal structures of the neutral complexes **2a**[39] and **4a**[40] with the corresponding symmetric ligands, **2** and **4**, have already been reported, which thus allows a comparison of their relevant structural features with those of **1a**.

The structural analysis of **1a** evidences the presence of only the *trans* isomer in the unit cell (Figure 5), in which the palladium ion attains a distorted square planar geometry with a relatively small bite angle (N1–Pd–N2 of 78.67(15)°).

In agreement with the *trans* influence of the Pd–CH_3 fragment, in all the three complexes **1a**, **2a**, and **4a** the Pd–N bond length *trans* to the Pd–C bond is longer than the other

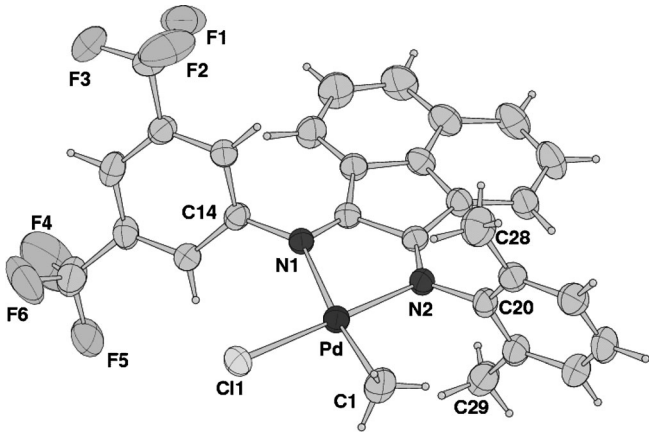

Figure 5. ORTEP drawing (thermal ellipsoids at the 40% probability level) of complex **1a**·2 $CHCl_3$. Of the disordered F1-3 group, only fluorines at higher occupancy are shown. Selected bond lengths (Å) and angles (°): Pd–C(1) 2.010(5), Pd–Cl(1) 2.2991(14), Pd–N(1) 2.201(4), Pd–N(2) 2.063(4), N(1)–Pd–N(2) 78.67(15), C(1)–Pd–Cl(1) 89.37(18), C(1)–Pd–N(1) 172.4(2), C(1)–Pd–N(2) 94.0(2), Cl(1)–Pd–N(1) 98.05(11), Cl(1)–Pd–N(2) 175.28(11).

Pd–N bond length. Within the standard deviation, the Pd–N1 bond lengths in **1a** and **2a** are similar (2.201(4) and 2.203(5) Å, respectively) and shorter than that in **4a** (2.227(4) Å), which suggests the lower coordinating capability of **4**; this is in agreement with the presence of electron-withdrawing groups on both the aryl rings. The Pd–N2 bond lengths in the three complexes are in the range of 2.052(3)–2.088(6) Å.

The orientation of the substituted phenyl rings in the three complexes is worth noting. The dihedral angles formed by 3,5-bis(trifluoromethyl)phenyl with the BIAN mean plane on the chlorido side are 64.5(1)° in **1a** and 53.3(1)° in **4a**, whereas the corresponding values for the phenyl *cis* to the Pd–CH_3 fragment are 80.1(1) and 78.3(2)°, respectively, which indicates a greater conformational freedom in the former case owing to a smaller bulk for the chlorido than for methyl. Contrarily, in **2a** the measured dihedral angles for the two 2,6-dimethylphenyl rings are very similar, 76.1(2) and 80.1(2)°, which thus confirms that the substituents in the *ortho* positions of both aryl rings hinder a tilt beyond a certain limit to avoid steric clashes.

The monocationic complex with acetonitrile, **1b**, was obtained by following the well-known method (Scheme 2).[41] The synthesis of the dimethyl sulfoxide derivatives, **1c**, **2c**, and **4c**, was achieved by a slight modification of the methodology applied for the acetonitrile complexes (Scheme 2; see the Experimental Section). Both the series of complexes were characterized by using ^1H and ^{13}C NMR spectroscopy in CD_2Cl_2.

The ^1H NMR spectrum of **1b** shows, at room temperature, sharp signals, as observed for Pd–acetonitrile derivatives with Ar-BIAN ligands[26]. The number of signals and their integration indicate the prevalence of the *trans* isomer; for **1b** the *trans*/*cis* ratio is 10:1, whereas for **1a** it is 19:1.

For the dimethyl sulfoxide derivatives, different NMR spectra are obtained depending on the nature of the Ar-BIAN ligand. In the ^1H NMR spectrum of **2c**, sharp signals are present at room temperature (Figure 6a). The chemical shift of the singlet of the methyl groups of dmso (at 2.89 ppm) indicates its coordination through the sulfur atom; other relevant signals are

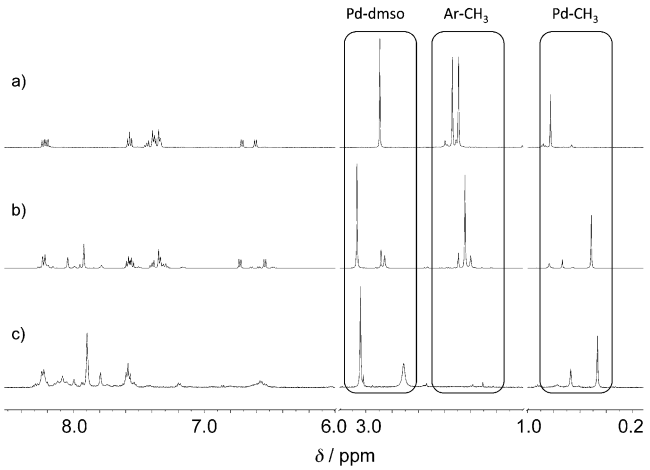

Figure 6. ^1H NMR spectra in CD_2Cl_2 of a) **2c** at $T = 298$ K, b) **1c** at $T = 233$ K, and c) **4c** at $T = 223$ K.

the two singlets at 2.34 and 2.29 ppm owing to the methyl groups on the aryl rings and the singlet at 0.83 ppm assigned to the Pd–CH_3 fragment. For complexes **1c** and **4c**, broad signals are observed at room temperature and they become sharper with the decrease in temperature. In the case of **4c**, the decoalescence of signals due to methylic protons was achieved at 223 K, which proved the presence of two species in the solution that differ in the coordination mode of dmso: the singlet at 3.04 ppm is attributed to S-bonded dmso and the singlet at 2.71 ppm is attributed to O-bonded dmso (Figures 6c and S1). Two singlets are also observed for the Pd–CH_3 group at 0.48 and 0.67 ppm. The two species are in the ratio 3:2, and the isomer with S-bonded dmso is the major species.

For complex **1c**, at the decoalescence temperature (233 K; Figures 6b and S2) the signals indicate the presence of three species in solution: one major and two minor species in 13:3:2 ratio.

In the NOESY spectrum of **1c** recorded at 233 K, cross peaks due to both exchange processes and Overhauser effect are observed (Figure S3). For the major species, the cross peak between the signal of the methyl group bonded to palladium (at 0.51 ppm) and the singlet of the methyl groups on the aryl ring of the ligand (at 2.24 ppm) indicates that this species is the *trans* isomer. The signal of the methyls of dmso at 3.07 ppm is indicative of dmso bonded to palladium through sulfur. Thus, the major species is featured by S-bonded dmso and the Pd–CH_3 fragment *trans* to the Pd–N bond of the aryl ring substituted with the CF_3 groups (species **i** in Scheme 3).

The characterization of two minor species was achieved by comparison with the spectra of **2c** and **4c** (Figure 6). The signals of **1c** at 2.88 ppm (CH_3 of dmso) and 2.29 ppm (aryl CH_3) have similar chemical shifts to those of **2c** and are therefore assigned to the species with the Pd–CH_3 group *trans* to the

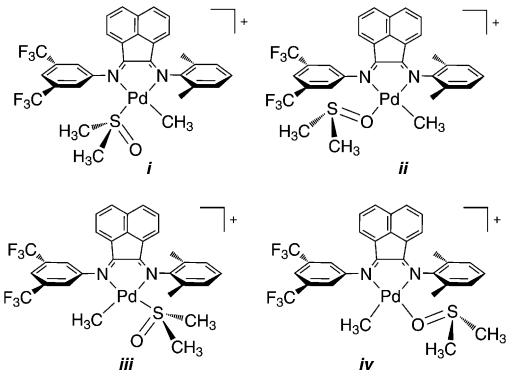

Scheme 3. Schematic representation of the four possible isomers for complex **1 c**.

CH_3-substituted ring (*cis* isomer) and S-bonded dmso (species **iii** in Scheme 3). The remaining singlets at 2.86 ppm (CH_3 of dmso) and 2.20 ppm (aryl CH_3) are attributed to the *trans* isomer with O-bonded dmso (species **ii** in Scheme 3). These attributions are unambiguously confirmed by ^1H–^{13}C HSQC experiments (Figure S4). Compared to free dmso, the carbon atoms resonate at a higher frequency if coordinated to a transition metal through sulfur and at a lower frequency if bonded through oxygen.[42] In the ^1H–^{13}C HSQC spectrum of **1 c**, both the major and one of the two minor species have the cross peak of dmso at higher frequency than that of free dmso whereas for the other minor isomer the dmso cross peak falls at a lower frequency, which thus confirms the previous assignments.

In addition, the singlets due to the Pd–CH_3 groups in the three isomers were assigned on the basis of the results of comparison of their ^{13}C chemical shift with that of the related complexes **2 c** and **4 c** with the symmetric Ar-BIANs.

Finally, as demonstrated by the cross peaks caused by exchange processes present in the NOESY spectrum, the three isomers of **1 c** are in equilibrium and at room temperature the rate of this exchange process is comparable to the NMR timescale. In the ^1H NMR spectrum of **1 c** recorded in [D_6]DMSO, sharp signals are already present at 298 K and indicate the presence of only one species (Figure S5). The chemical shift of the Pd–CH_3 signal indicates that this species is species **i** (Scheme 3). This experiment indicates that the dynamic process that exchanges species **i**, **ii**, and **iii** occurs through an associative mechanism.

The different coordination mode of dmso was also confirmed in the solid state by the stretching frequency of the S–O bond in the IR spectra: one band typical of S-bonded dmso is observed in the IR spectrum of **2 c**, whereas two bands at the bands of S- and O-bonded dmso, respectively, are present in the IR spectra of **1 c** and **4 c**.

Thus, for complex **1 c**, only three of the four possible isomers are observed (Scheme 3).

By simple considerations about coordination chemistry, the major isomer (species **i** in Scheme 3) should be the most stable: dmso is bonded through sulfur (soft base) to Pd^{2+} (soft acid); the Pd–CH_3 bond is *trans* to the Pd–N bond of the nitrogen atom with lower Lewis basicity. Contrarily, isomer **iv** (Scheme 3), with dmso bonded through oxygen (hard base) to Pd^{2+} (soft acid) and the coordinated methyl competing with the *trans* located N-donor atom of higher Lewis basicity, should be the least stable and was not detected. The stability of the other two species, **ii** and **iii**, should lie in between that of **i** and **iv**.

The observation that the *trans* isomer is the prevailing species in all the cases is in agreement with the literature data, which indicate a preferential tendency for the methyl group to be coordinated *trans* to the lower basic N atom in Pd–methyl complexes of electronically unequivalent N-donor atoms.[41,43–46] The opposite situation is observed for palladium complexes in which steric requirements overcome the electronically driven coordination.[47]

Ethylene/MA cooligomerization and mechanistic studies

Complexes **1 b**–**5 b**, **1 c**, **2 c**, and **4 c** were tested as precatalysts for ethylene/MA cooligomerization by performing the reaction in 2,2,2-trifluoroethanol as solvent at $T = 308$ K and $P_{C_2H_4} = 2.5$ bar (1 bar = 0.1 MPa) for 24 h (Scheme 4). The catalytic

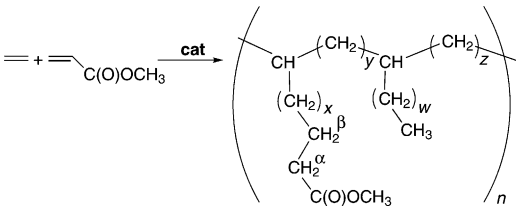

Scheme 4. Ethylene/methyl acrylate cooligomerization.

product was a yellow-red oil, which was characterized by using ^1H and ^{13}C NMR spectroscopy. In addition, a small portion of the reaction mixture, before the workup, was analyzed by using GC–MS to determine whether higher alkenes were also formed.

Precatalysts **3 b**–**5 b** with symmetrically substituted ^{m}Ar-BIANs coordinated to palladium were found practically inactive, which yielded an oil that contained palladium derivatives, ethylene/MA cooligomers, and higher alkenes (Table 1, runs 1–3). This inactivity is related to the fast decomposition of the catalyst to inactive palladium metal that formed within the first 4 h of the reaction. Contrarily, precatalyst **1 b** with the nonsymmetric ligand **1** was found more productive than **2 b**, which is considered as the reference compound with the symmetric Ar-BIAN substituted on the *ortho* positions; the obtained catalytic product contains a slightly higher amount of polar monomer (Table 1, runs 4 and 5). An increase in productivity was achieved with the Pd–dmso derivatives; on average, the productivity of **1 b** and **1 c** was two times higher than that of **2 b** and **2 c**, respectively (Table 1, runs 4–8). A slight decrease in the content of the polar monomer incorporated into the catalytic product was found with use of the Pd–dmso derivatives instead of the Pd–acetonitrile compounds. However, at least in some cases, this decrease can be attributed to the

Table 1. Ethylene/methyl acrylate cooligomerization: effect of the Ar-BIAN ligand.[a]

Run	Precatalyst	L	Yield [mg]	g P/g Pd[b]	Mol% MA[c]	Bd[c,d]	Alkenes
1	**3b**	CH_3CN	56.7[e]				C4–C6
2	**4b**	CH_3CN	37.1[e]				C4–C6
3	**5b**	CH_3CN	19.3[e]				C4–C6
4	**2b**	CH_3CN	171.4	79.4	10.4	101	–
5	**1b**	CH_3CN	297.0	133.2	14.7	137	C4–C16
6	**2c**	dmso	221.8	99.5	6.6	117	–
7	**4c**	dmso	55.0[e]				C4–C6
8	**1c**	dmso	520.8	233.5	12.5	146	C4–C16
9[f]	**2b+4b**	CH_3CN	73.6	33.0	8.1	119	–

[a] Precatalyst: $[Pd(CH_3)(L)(Ar\text{-}BIAN)][PF_6]$. Reaction conditions: $n_{Pd} = 2.1 \times 10^{-5}$ mol, 2,2,2-trifluoroethanol: $V = 21$ mL, $T = 308$ K, $P_{C_2H_4} = 2.5$ bar; methyl acrylate (MA) $V = 1.13$ mL, [MA]/[Pd] = 616, $t = 24$ h; [b] Isolated yield; g P/g Pd = grams of product per gram of palladium; [c] Calculated by using ^1H NMR spectroscopy (see the Supporting Information); [d] Bd = degree of branching as branches per 1000 carbon atoms; $C(O)OCH_3$ carbon atoms are excluded; [e] Mixture of palladium derivatives, ethylene/methyl acrylate cooligomers and higher alkenes; [f] $n_{2b} = n_{4b} = 1.05 \times 10^{-5}$ mol.

higher MA conversion in the reaction of the former catalysts than in the reaction of the latter ones, as discussed later in more detail.

In agreement with Brookhart's system,[10,11] for precatalysts **2b** and **2c**, no higher alkenes were formed whereas in all other cases butenes and hexenes were also obtained, and for complexes **1b** and **1c** the produced alkenes ranged from C4 to C12 with traces of C14 and C16 (Table 1, Figures S6–S8). The formed alkenes are a complex mixture of isomers as the result of the chain walking mechanism.[8] The observed chain length distribution, expressed in terms of molar fraction of each alkene, can be reasonably fitted by the Poisson distribution (see the Supporting Information). With precatalysts **1b** and **1c**, the product with the higher concentration is C6 whereas the product with the higher weight fraction is C8.

The observed formation of higher alkenes with the symmetrically substituted ^{m}Ar-BIANs is due to the lack of steric hindrance on the *ortho* positions of the aryl rings that does not avoid the β-hydrogen elimination.[8,48] In the case of catalysts with ligand **1** with one aryl ring substituted on both *ortho* positions and the other ring substituted on both *meta* positions, β-hydrogen elimination is slowed down slightly and longer alkenes were produced. These data highlight the subtle role played by the position of the substituents on the ancillary ligand in regulating the length of the synthesized macromolecules.

As far as the effect of the nature of the Ar-BIAN ligand on the productivity is concerned, which is in agreement with the data reported for the CO/vinyl arene copolymerization,[26] even for the currently investigated reaction, the catalyst with the nonsymmetric ligand bonded to the metal center is more productive than those with the corresponding symmetric Ar-BIANs for both the Pd–$NCCH_3$ and Pd–dmso derivatives (Table 1, **1b** vs. **2b** and **4b**, **1c** vs. **2c** and **4c**).

A catalytic experiment was performed by using a 1:1 mixture of precatalysts **2b** and **4b**, which yielded a productivity much lower than that obtained with **1b**; this indicates that no scrambling process occurs during catalysis with the latter (Table 1, run 9). The value of productivity, the acrylate content, and the lack of higher alkenes in the product indicate that active species is originated by **2b**.

By applying precatalysts with ligand **1**, the effect of reaction parameters, such as temperature, ethylene pressure, and reaction time, was investigated. Productivity increases on increasing the temperature from 298 to 308 K for **1c**, whereas it decreases slightly for **1b**. For both precatalysts, an increase in temperature up to 318 K results in a sharp decrease in productivity owing to the decomposition of the catalysts to inactive palladium metal, which indicates their low thermal stability (Figure 7).

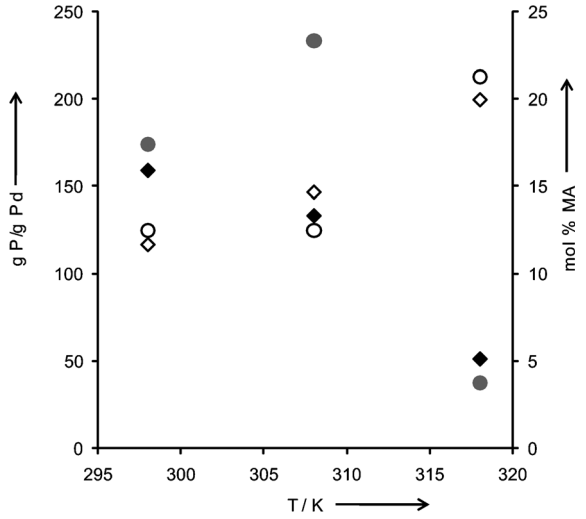

Figure 7. Ethylene/methyl acrylate cooligomerization: effect of temperature. Precatalyst: $[Pd(CH_3)(L)(\mathbf{1})][PF_6]$ (L = CH_3CN, dmso). Reaction conditions: see Table 1. Filled symbols: productivity data; open symbols: mol% MA: **1b** (◆,◇); **1c** (●,○).

An increase in the content of the incorporated polar monomer into the catalytic product is achieved by increasing the temperature for both catalysts. Even the production of alkenes shows a progressive decrease, more pronounced for **1c**, moving from 298 to 318 K (Figure S6).

The effect of ethylene pressure was studied in the range 1.5–7.0 bar (Figure 8).

For both precatalysts, productivity increases on increasing ethylene pressure up to 5.0 bar; however, an increase in pressure up to 7.0 bar results in a less pronounced increase in productivity. In the case of **1c**, the value of 400 g P/g Pd is reached at 7.0 bar. As expected,[10,11] the increase in ethylene pressure results in a progressive decrease in the content of the polar monomer incorporated in the catalytic product (Figure 8). The ethylene pressure significantly affects the production of higher alkenes (Figure S7). Their amount increases continuously from 1.5 to 7.0 bar, with a slight shift to higher alkenes in the Poisson distribution.

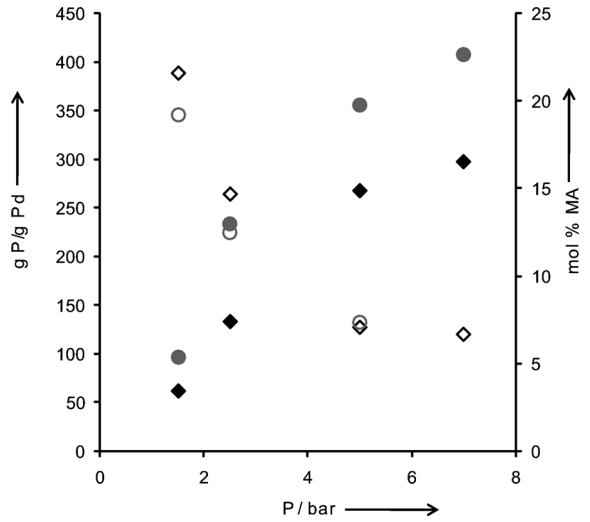

Figure 8. Ethylene/methyl acrylate cooligomerization: effect of pressure. Precatalyst: $[Pd(CH_3)(L)(\mathbf{1})][PF_6]$. Reaction conditions: see Table 1. Filled symbols: productivity data; open symbols: mol% MA: **1b** (◆,◇); **1c** (●,○).

A different catalytic behavior of the two precatalysts **1c** and **1b** is observed by evaluating the effect of the reaction time by conducting the catalytic experiments at $P_{C_2H_4} = 2.5$ bar and $T = 308$ K (Figure 9).

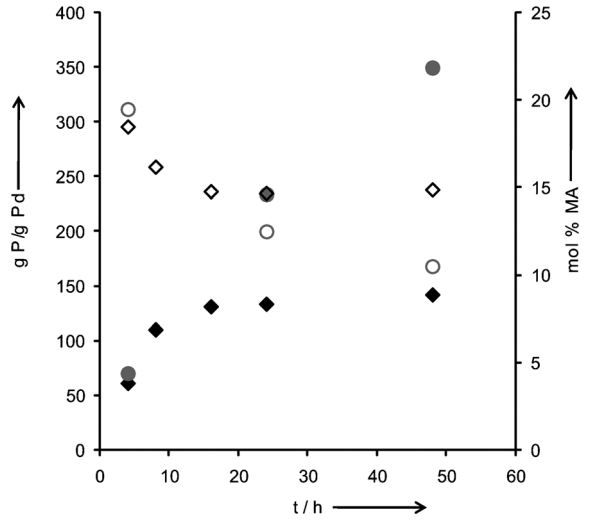

Figure 9. Ethylene/methyl acrylate cooligomerization: effect of reaction time. Precatalyst: $[Pd(CH_3)(L)(\mathbf{1})][PF_6]$. Reaction conditions: see Table 1. Filled symbols: productivity data; open symbols: mol% MA: **1b** (◆,◇); **1c** (●,○).

Although precatalyst **1b**, with acetonitrile as the labile ligand, is deactivated within 16 h of the reaction, precatalyst **1c** is active for at least 48 h, which reaches a productivity of approximately 350 g P/g Pd. Only a partial decrease in productivity is apparent at a long reaction time, which can be partly explained by the kinetics of the reaction, as detailed in the following. The longer catalyst lifetime for **1c** indicates that the better performing catalytic behavior of the precatalyst with dimethyl sulfoxide than that with acetonitrile could be not only due to the lower coordinating capability of dmso with respect to CH_3CN, but also due to additional reasons (described below). As also shown in Figure 9, the percentage of MA incorporated in the oligomer decreases as the reaction proceeds. This can also be explained, at least qualitatively, on the basis of the reaction kinetics (described below). An unusual effect of the reaction time was observed on the production of higher alkenes (Figure S8). A progressive increase in their amounts, together with an increase in the average chain length *k*, was observed up to 16 h. When the reaction was stopped after 24 h, the concentration of alkenes decreased drastically; however, when the reaction was continued up to 48 h, it became higher again, but with low *k* values. This peculiar behavior could be rationalized by considering the main processes operative in solutions. The ethylene oligomerization results in the increase in concentration and in the lengthening of the alkene chains (*k* values). At the same time, the reaction with MA results in the consumption of alkenes and in the formation of cooligomers. As the concentration of alkenes increases, the possible insertion of higher alkenes instead of ethylene cannot be excluded. At the lower reaction times, the predominant processes are ethylene oligomerization and ethylene/MA cooligomerization. As the reaction proceeds, formed alkenes participate in the cooligomerization process, which results in the decrease in their concentration. With the increase in the reaction time, MA concentration decreases and, below a critical value, ethylene oligomerization becomes the predominant process, which produces a higher amount of higher alkenes.

The characterization of the isolated catalytic product was performed by using ^1H and ^{13}C NMR spectroscopy in $CDCl_3$ solution at room temperature. The signals in the spectra were identified by comparison with literature data[8,12,14,49–52] and by multidimensional homo- and heteronuclear NMR experiments (Figures S9–S12). In the ^1H NMR spectra of the oils synthesized with precatalysts **1b** and **1c**, the following signals are recognized: the signals at 5.60–4.90 ppm assigned to the vinylic protons, the singlet at 3.60 ppm assigned to the methoxy group, the broad signals between 2.50 and 1.50 ppm assigned to allylic protons and to methylenic groups close to MA units, the broad signal centered at 1.23 ppm assigned to the methylenic and methynic moieties of ethylene units, and the signals between 1.0 and 0.6 ppm assigned to methyl groups at the end of branches (Figure 10). No signal due to methynic carbon atoms of MA units was observed.

The NMR analysis indicates that both ethylene oligomers and ethylene/MA cooligomers are highly branched ($\approx$100 branches per 1000 carbon atoms; Table 1) and the polar monomer is inserted at the end of the branches as the $-CH_2-CH_2-C(O)OCH_3$ fragment, which is the result of the chain walking mechanism; this is in agreement with Brookhart's system.[10,11] From the NMR analysis, the presence of higher alkenes in the isolated catalytic product cannot be excluded.

To gain some insights into the reactions involved in the catalytic cycle, the independent reactivity of the two comonomers with complexes **1b**, **2b**, and **4b** was investigated by using in situ NMR spectroscopy. A 10 mM CD_2Cl_2 solution of **1b** was reacted with ethylene at room temperature. In the ^1H NMR spectrum recorded after 10 min of the bubbling of the apolar

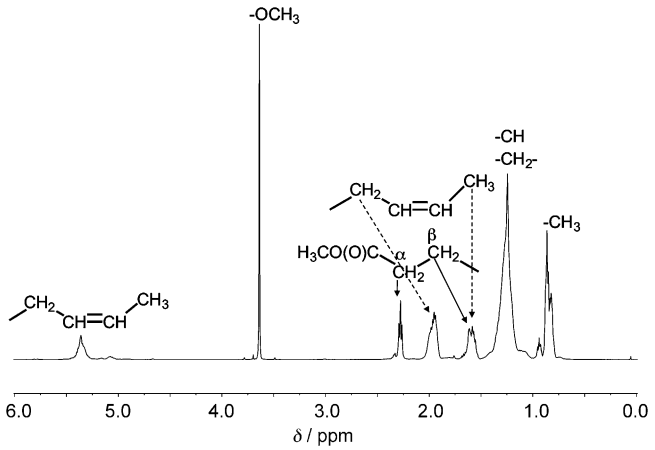

Figure 10. ^{1}H NMR spectrum in $CDCl_3$ at 298 K of the ethylene/methyl acrylate cooligomers obtained with **1 c** (analogous spectrum for ethylene/methyl acrylate cooligomers obtained with **1 b**).

monomer, no signal of the precursor was present and the signals of butenes and hexenes were observed. The fast reactivity of **1 b** with alkene is in agreement with Brookhart's system.[11,48]

The reactivity with MA was investigated by adding 2 equiv of the polar monomer to the 10 mM CD_2Cl_2 solution of the complex at room temperature. The ^{1}H NMR spectra were recorded every 5 min for the first 20 min after the addition of the polar monomer. The three complexes showed the same behavior: in the first spectrum recorded after the addition of MA, the signals of the precatalyst were present together with the new signals assigned to the five- and six-membered palladacycles **B"** and **C"** (Scheme 5; Figures S13–S15). In addition, the signal of free acetonitrile was present and the resonances of **A'** were observed at longer reaction times. The reactivity of the three complexes differs with the rate of the reaction, which decreases in the order **4 b** > **2 b** > **1 b** (Figures 11 and S16). The different trend of reactivity with respect to that of productivity is related to the different stabilities of the three catalysts: **4 b** is the fastest but least stable, and **1 b** is the slowest but very stable.

The rate of the reaction of the precatalyst with MA follows a first-order kinetic. The same is likely to hold for the related insertion of MA into the growing oligomer chain. Because during the catalytic reactions ethylene pressure is kept constant, the apparent rate dependence on ethylene pressure will be pseudo zero order for any single reaction. (For ethylene polymerization catalyzed by Brookhart's system, a zero-order rate of ethylene disappearance was modeled.)[8] We plan to perform a series of kinetic experiments to prove or disprove these assumptions, and those will be published in a future paper. However, we note that these reasonable assumptions allow us to justify some of the trends evidenced previously.

1. *The productivity of the catalyst decreases with reaction time even in the case of the Pd–dmso complex* ***1 c***. From the amount of the product obtained and the percentage of MA measured by using NMR spectroscopy, it is easy to calculate the moles of MA and ethylene consumed for each reaction (see Supporting Information for the details). This allows us to treat the MA and ethylene consumption separately, which is in agreement with the presence of two processes: ethylene oligomerization and ethylene/MA cooligomerization. The data for the reactions cat-

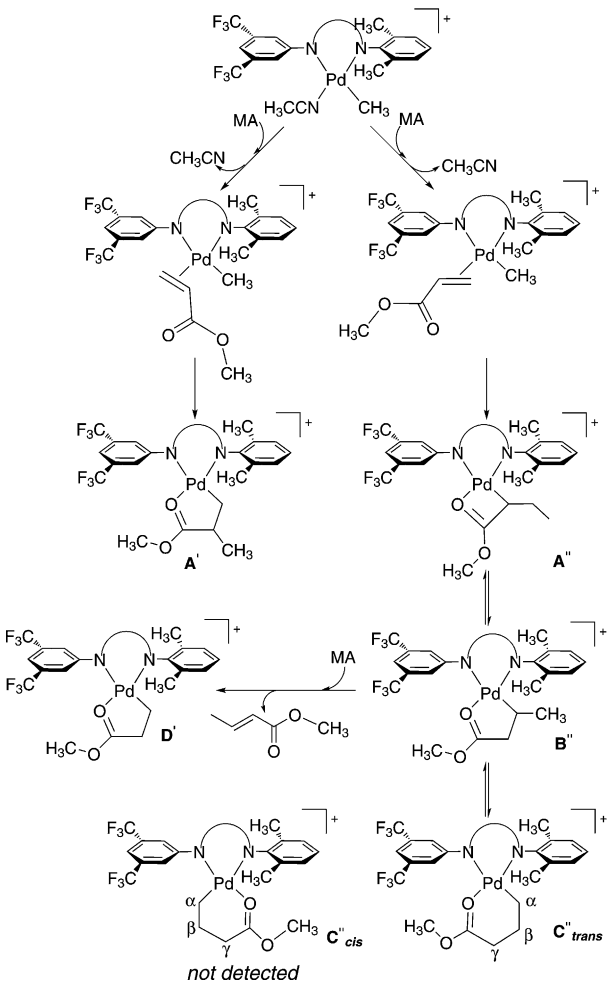

Scheme 5. Proposed reaction mechanism for the reactivity of complex **1 b** with methyl acrylate.

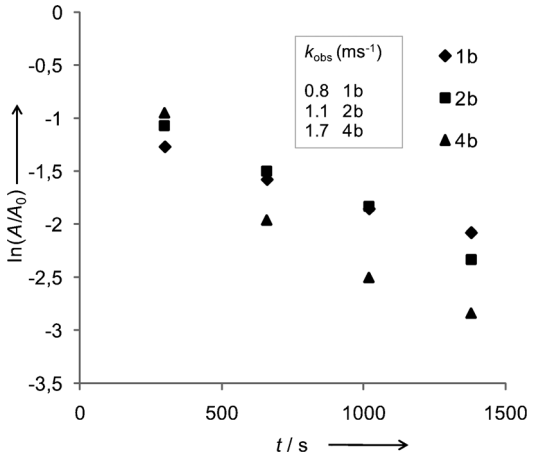

Figure 11. First-order rate for the consumption of Pd–CH_3 by insertion of methyl acrylate ([Pd] = 10 mM in CD_2Cl_2, T = 298 K, $A = [Pd–CH_3]_t$, $A_0 = [Pd–CH_3]_{t=0}$).

alyzed by **1c** can be fitted quite well by a kinetic model, which is first order in MA and pseudo zero order in ethylene. A small decrease in activity can be observed, which must be attributed to some catalyst deactivation; however, most of the decrease in productivity at long reaction times can be attributed to the slowing down of the MA insertion owing to the consumption of the MA. Contrarily, in the case of the reactions catalyzed by **1b**, the model fails completely. In this case, catalyst deactivation is clearly the main reason for the decrease in productivity with time.

2. *The percentage of MA in the product decreases as the reaction proceeds.* The insertion reactions of MA and ethylene compete with each other. To a first approximation, it can be assumed that the relative insertion rate is proportional to the MA/ethylene ratio in solution. Because the concentration of MA decreases during the reaction but that of ethylene does not, it is to be expected that the percentage of inserted MA will decrease at higher MA conversions, such as those that occur if the reaction time is increased, at least for the Pd–dmso catalysts. Although we tried to model quantitatively the product composition on the basis of this principle, the limited amount of data makes the conclusions unreliable. However, on a semiquantitative basis, we can confirm that the product composition roughly follows the expected trend.

3. *The rate does not increase linearly with ethylene pressure, and the percentage of MA insertion decreases along the series.* The reason for this is immediately clear from what is said above. An increase in ethylene pressure increases only the rate of ethylene insertion. It does not increase the rate of MA insertion. Because the productivity of the catalyst is due to the sum of two insertions, a linear increase in productivity with ethylene pressure is not to be expected under any circumstance. Contrarily, a higher ethylene pressure increases the ethylene/MA ratio in solution and makes the MA insertion less competitive.

The NMR studies described above also allow us to propose a more detailed hypothesis for the mechanism of the reactivity with MA (Scheme 5). The substitution reaction of acetonitrile with the polar monomer takes place on the precatalyst, which leads to free acetonitrile and two intermediates that differ in MA orientation. On these intermediates, the migratory insertion of the polar monomer into the Pd–CH_3 bond takes place with primary and secondary regiochemistry, respectively; the latter is remarkably favored. The insertion with primary regiochemistry leads directly to the five-membered palladacycle **A'**, whereas in the case of the insertion with secondary regiochemistry, the detected six-membered metallacycle **C"** is the result of the chain walking mechanism. The insertion of the polar monomer into the Pd–CH_3 bond with secondary regiochemistry is typical for MA, which is observed in palladium complexes with α-diimines,[10] phosphine sulfonate derivatives, phosphino acetamido-derived ligands,[53] and (phosphinomethyl)oxazoline P–N ligands.[54] The insertion with exclusively primary regiochemistry was instead observed for methyl methacrylate on Pd–α-diimine complexes.[55]

For complex **1b**, the reactivity with MA was followed up to 17 h, which indicated the disappearance of the signals attributed to the two metallacycles **B"** and **C"** and the appearance of the resonances of methyl crotonate (**A'**) and of **D'** (Figure S17). Methyl crotonate is the result of β-hydrogen elimination on the five-membered palladacycle **B"** (Scheme 5). **C"** and **B"** are in equilibrium as probed by the cross peaks due to exchange processes present in the NOESY spectrum (Figure S18, cross peak in green circle). **D'** is the result of the migratory insertion of MA into the Pd–H bond. This intermediate was also observed in Brookhart's system.[10]

Notably, in the case of the intermediates with the nonsymmetric ligand **1**, *cis* and *trans* isomers are possible. As reported above, the *trans* isomer is featured by the Pd–C bond *trans* to the Pd–N bond of the *meta*-substituted ring. In the ^{1}H NMR spectra, the signals of only one isomer are evident for **C"** (Figure S13; the concentrations of **A'** and **B"** are too low to allow the detection of their other possible isomers). Their assignment was based on the following criteria: (1) The intensity of the singlet of the aryl CH_3 of **1b** decreases as the reaction proceeds, and this singlet is replaced by a new singlet at a higher frequency (2.32 ppm; Figure S13). (2) The signal of H^3 on the acenaphthene skeleton is also shifted at a higher frequency (7.24 ppm). (3) The signals of $H^{14,16,18}$ overlap, whereas they are separated in the precursor. (4) A clear cross peak between the aryl CH_3 and the Pd–CH_2^{α} of **C"** is present in the NOESY spectrum (Figure S18, cross peak in black circle). (5) No variation is observed in the chemical shift of H^{10}. All these NMR data indicate that the *trans* isomer (**C"**$_{trans}$) is the only one present, which thus suggests that after the migratory insertion of MA, the isomerization of the growing chain occurs.

During catalysis, in the growing of the cooligomer chain the metallacycle **C"**$_{trans}$ could also be responsible for the formation of the –CH_2–CH_2–C(O)OCH_3 fragment. In a preliminary in situ NMR experiment, complex **1c**, with dmso bonded to palladium, is reacted with 2 equiv of MA. In the ^{1}H NMR spectrum recorded after 2 min of the addition of MA, no signal of **1c** is present and the signals of **B"** and **C"**$_{trans}$ are observed together with a broad peak at 2.63 ppm; no signal of free dmso is evident. Following the reaction with time, the signal at 2.63 ppm increases in intensity and becomes sharper. In addition, the typical signals of the metallacycles **B"** and **C"**$_{trans}$ fall at a frequency slightly different from that of the same signals observed for the reactivity of **1b** (Figure S19). These signals are tentatively assigned to an open intermediate analogous to **C"**$_{trans}$ with dmso bonded to palladium instead of the oxygen atom of the inserted MA unit. In a paper by Mecking on Pd–phosphine sulfonate complexes,[28] the effect of coordinating ligand L, such as dmso and various phosphine oxides, on the ethylene/MA copolymerization activity and on the rate of monomer insertion has been investigated. It has been demonstrated that the coordination strength of dmso exceeds that of the oxygen atom of the carbonyl group of the polar monomer in a four-membered intermediate analogous to **A"**. The open intermediate resulting from the insertion of MA into the Pd–CH_3 bond and with coordinated dmso, [Pd{CH($COOCH_3$)CH_2CH_3}(dmso)(P–O)], that corresponds to the open form of **A"** was isolated from the reaction of MA with [Pd(CH_3)(dmso)(P–O)].[14] In the Pd–(P–O) catalytic system, no chain

walking mechanism occurs and, thus, dmso competes favorably with the oxygen atom of the four-membered palladacycle analogous to **A"** whereas in the Pd–α-diimine system, dmso has to compete with the oxygen atom of the six-membered metallacycle **C"**, which is more difficult to open than **A"**.

Our preliminary investigation indicates that the different catalytic behavior of Pd–$NCCH_3$ and Pd–dmso derivatives could be attributed to the capability of dmso to remain coordinated to palladium in the apical position of a pentacoordinated intermediate, which thus competes with the oxygen atom of the last inserted MA unit and favors the opening of the metallacycle **C"**$_{trans}$—the resting state of the catalytic cycle—and the insertion of the next incoming monomer. The DFT calculation showed that in the palladium-catalyzed carbon monoxide/ethylene copolymerization, carbon monoxide and ethylene exchange through an associative mechanism via a trigonal bipyramidal intermediate.[56] Further investigations are in progress.

Conclusions

The synthesis and characterization of a peculiar nonsymmetrically substituted bis(aryl-imino)acenaphthene (Ar-BIAN) ligand is reported. This ligand and the corresponding symmetrically substituted derivatives are used to synthesize the relevant neutral and monocationic Pd–methyl complexes. The series of the monocationic complexes has been extended to the dimethyl sulfoxide derivatives, and this is the first report on Pd–dmso compounds with α-diimines as ancillary ligands. The characterization of the Pd–dmso compounds probes the presence of different species in solution depending on Ar-BIAN: for ligand **2**, only the compound with S-bonded dmso is observed; for ligand **4**, both isomers with S- and O-bonded dmso are present; for ligand **1**, three species are observed that differ in the coordination mode of dmso and the relative position of Pd–CH_3 with respect to the two halves of Ar-BIAN.

Both the Pd–$NCCH_3$ and Pd–dmso complexes with the new nonsymmetric Ar-BIAN ligand are tested as precatalysts in the ethylene/methyl acrylate cooligomerization with regard to the catalytic behavior of the complexes with the corresponding symmetric Ar-BIANs under mild reaction conditions of temperature and ethylene pressure. The catalytic product is a mixture of ethylene/methyl acrylate cooligomers and higher alkenes. The catalysts containing the nonsymmetric Ar-BIAN ligand are found to be more productive than those containing the symmetric counterparts, yielding the cooligomer with a higher content of the polar monomer, which thus supports the idea that a subtle unbalance of the steric and electronic properties of the ancillary ligand has a positive effect on the catalytic performances.

For all the tested ligands, the catalysts obtained from the Pd–dmso derivatives were found to be more productive than those obtained from the Pd–$NCCH_3$ derivatives. The higher productivity of the Pd–dmso catalysts was observed in both the isolated product and the higher alkenes production. The Pd–dmso catalyst with ligand **1** showed a longer lifetime than the corresponding Pd–$NCCH_3$ derivative. In situ NMR investigations indicate that the higher stability of the Pd–dmso catalyst could be related to the possibility of dimethyl sulfoxide competing with the oxygen atom of the last inserted MA unit, which favors the cleavage of the Pd–O bond and the insertion of the new incoming monomer.

Further investigations aiming at evaluating the capability of dmso to stabilize the catalytically active species are currently in progress.

Experimental Section

General considerations

All complex manipulations were performed by using standard Schlenk techniques under argon. Anhydrous dichloromethane was obtained by distilling it over CaH_2 and under argon. Before use, $ZnCl_2$ and basic Al_2O_3 were stored in an oven at 110 °C overnight. Ligands **2**–**4**,[30,57] **5**,[26] [Pd(CH_3)Cl(cod)], their neutral palladium complexes, and acetonitrile derivatives[41] were synthesized according to methods given in the literature. [Pd($OAc)_2$] was donated by Engelhard Italia and used as received. Ethylene (purity ≥ 99.9%) supplied by SIAD and MA (99.9%, with 0.02% of hydroquinone monomethyl ether) supplied by Aldrich were used as received. Deuterated solvents were stored as recommended by Cambridge Isotope Laboratories. All the other reagents and solvents were purchased from Sigma–Aldrich and used without further purification for synthetic, spectroscopic, and catalytic purposes.

The NMR spectra of ligands, complexes, and catalytic products and of the in situ reactivity investigations were recorded by using a Varian 500 MHz spectrometer at the following frequencies: 500 MHz (^{1}H) and 126 MHz (^{13}C); the resonances (δ) were reported in ppm and referenced to the residual solvent peak versus Si(CH_3)$_4$: $CDCl_3$ at δ 7.26 (^{1}H) and δ 77.0 (^{13}C), CD_2Cl_2 at δ 5.32 (^{1}H) and δ 54.0 (^{13}C), and [D_6]DMSO at δ 2.50 (^{1}H) and δ 39.5 (^{13}C). NMR experiments were performed by using the automatic software parameters; in the case of NOESY and ROESY experiments, a mixing time of 500 and 250 ms was used, respectively. In situ kinetic investigations were performed by using the pre-acquisition delay (pad) Varian experiment.

IR spectra were recorded in Nujol by using a Perkin–Elmer System 2000 FT-IR spectrometer. Elemental analyses were performed in the analytical laboratories of the University of Udine. The mass spectra of ligand **1** and complexes were run by ESI ion trap by using a Bruker Esquire 4000. GC–MS analyses were performed with an Agilent 7890 GC using a DB-225 ms column (J&W: 60 m, 0.25 mm inner diameter, 0.25 μm film) and helium as carrier coupled with a 5975 Series MSD. Before analysis, samples were diluted with methanol and nonane was added as the internal standard.

Synthesis of ligand 1

Ligand **1** was synthesized through the transimination reaction by using a method slightly different from that given in the literature.[29] [$ZnCl_2$(**4**)] (1.00 g, 1.35 mmol) was dissolved in CH_3OH (100 mL). To the orange solution 2,6-dimethyl aniline (366 μL, 2.97 mmol) was added, and the reaction mixture was stirred at RT for at least 7 days. The reaction was followed by TLC (alumina, hexane/diethyl ether = 2:1), and a final check was performed by using ^{1}H NMR spectroscopy. To do so, an aliquot of the solution was withdrawn and ligand decoordination was performed on it (see later). The reaction did not proceed over 50% of conversion. When it was reached, the yellow precipitate of [$ZnCl_2$(**2**)] and

[$ZnCl_2$(**4**)] was filtered off and the solution was concentrated to half volume and poured into a separating funnel together with CH_2Cl_2 (30 mL) and a water solution supersaturated with $Na_2C_2O_4$ (10 mL). The two phases were shaken for approximately 1 min until the organic phase color changed from yellow-orange to red-orange. The water phase was washed with CH_2Cl_2 (10 mL), and the two organic phases were combined, washed with water (2× 10 mL), dried over Na_2SO_4, and concentrated at reduced pressure to yield a red oil. The oil contained 2,6-dimethyl aniline, 3,5-bis(trifluoromethyl) aniline, and minor byproducts (e.g., monoketoimine), and it was purified by using column chromatography over basic alumina with hexane/diethyl ether (2:1) as eluent. Ligand **1** eluted first as an orange band (316.3 mg, 0.64 mmol).

[3,5-$(CF_3)_2C_6H_3$],[2,6-$(CH_3)_2C_6H_3$]BIAN (1)

Yield: 47%; MS (ESI): *m/z* (%): 519.2 (100) $[M+Na]^+$, 497.2 (80) $[M+H]^+$; found: C 66.94, H 3.45, N 5.24; elemental analysis calcd (%) for $C_{28}H_{18}N_2F_6$: C 67.74, H 3.65, N 5.64; isomeric ratio (*E,E*)/(*E,Z*): $CDCl_3$, 298 K: 2/1; CD_2Cl_2, 298 K: 1/1.

^{1}H NMR (500 MHz, $CDCl_3$, 298 K): Major isomer (*E,E*): $\delta = 7.98$ (d, $^3J = 8.3$ Hz, 1H; H^5), 7.94 (d, $^3J = 8.3$ Hz, 1H; H^8), 7.79 (s, 1H; H^{16}), 7.65 (s, 2H; $H^{14,18}$), 7.47–7.41 (m, 2H; $H^{4,9}$), 7.19–7.15 (m, 2H; $H^{15',17'}$), 7.13–7.07 (m, 1H; $H^{16'}$), 6.84 (d, $^3J = 7.2$, 1H; H^3), 6.73 (d, $^3J = 7.2$, 1H; H^{10}), 2.13 ppm (s, 3H; CH_3). Minor isomer (*E,Z*): $\delta = 8.16$ (d, $^3J = 7.1$, 1H; H^3), 8.07 (d, $^3J = 8.2$, 1H; H^5), 7.96 (d, $^3J = 8.2$, 1H; H^8), 7.82 (dd, $^3J = 8.2$, 7.1, 1H; H^4), 7.53 (s, 1H; H^{16}), 7.45 (s, 2H; $H^{14,18}$), 7.35 (dd, $^3J = 8.2$, 7.1, 1H; H^9), 7.07–7.02 (m, 1H; $H^{16'}$), 7.01–6.94 (m, 2H; $H^{15',17'}$), 6.53 (d, $^3J = 7.1$, 1H; H^{10}), 1.82 ppm (s, 3H; CH_3).

^{1}H NMR (500 MHz, CD_2Cl_2, 298 K): (*E,E*) isomer: $\delta = 7.99$ (d, $^3J = 8.3$ Hz, 1H; H^5), 7.96 (d, $^3J = 8.3$ Hz, 1H; H^8), 7.87–7.80 (m, 1H; H^{16}), 7.66 (s, 2H; $H^{14,18}$), 7.43 (m, 2H; $H^{4,9}$), 7.19 (d, $^3J = 7.4$ Hz, 2H; $H^{15',17'}$), 7.10 (t, $^3J = 7.4$ Hz, 1H; $H^{16'}$), 6.81 (d, $^3J = 7.3$ Hz, 1H; H^3), 6.72 (d, $^3J = 7.3$ Hz, 1H; H^{10}), 2.10 ppm (s, 3H; CH_3). (*E,Z*) isomer: $\delta = 8.16$ (d, $^3J = 7.0$ Hz, 1H; H^3), 8.10 (d, $^3J = 8.3$ Hz, 1H; H^5), 7.99 (d, $^3J = 8.3$ Hz, 1H; H^8), 7.87–7.80 (m, 1H; H^4), 7.56 (s, 1H; H^{16}), 7.48 (s, 2H; $H^{14,18}$), 7.37 (t, $^3J = 7.8$ Hz, 1H; H^9), 7.04 (m, 2H; $H^{15',17'}$), 6.98 (m, 1H; $H^{16'}$), 6.55 (d, $^3J = 7.1$ Hz, 1H; H^{10}), 1.81 ppm (s, 3H; CH_3).

^{13}C NMR (126 MHz, CD_2Cl_2, 298 K): $\delta = 130.0$ ($C^{5,8}{}_{E,Z}$), 129.8 ($C^{5,8}{}_{E,E}$), 129.1 ($C^{4}{}_{E,Z}$), 129.0 ($C^{9}{}_{E,Z}$ and $C^{15',17'}{}_{E,E}$), 128.7 ($C^{15',17'}{}_{E,Z}$ and $C^{4\text{ or }9}{}_{E,E}$), 128.2 ($C^{4\text{ or }9}{}_{E,E}$), 124.5 ($C^{16'}{}_{E,Z}$ and $C^{16'}{}_{E,E}$), 124.1 ($C^{3}{}_{E,E}$), 123.4 ($C^{10}{}_{E,E}$), 123.3 ($C^{10}{}_{E,Z}$), 120.9 ($C^{3}{}_{E,Z}$), 119.6 ($C^{14,18}{}_{E,E}$), 119.0 ($C^{14,18}{}_{E,Z}$), 118.3 ($C^{16}{}_{E,E}$), 116.9 ($C^{16}{}_{E,Z}$), 18.2 ($CH_3{}_{E,E}$), 17.8 ppm ($CH_3{}_{E,Z}$).

Synthesis of [$Pd(CH_3)Cl$(1)] (1 a)

[$Pd(CH_3)Cl$(cod)] (201.5 mg, 0.76 mmol) was kept in a Schlenk flask and dissolved in CH_2Cl_2 (3 mL). A solution of ligand **1** (417.0 mg, 0.84 mmol) in CH_2Cl_2 (3 mL) was added. The reaction mixture was protected from light, stirred at RT for 45 min, and then concentrated at half volume under reduced pressure. Upon addition of petroleum ether (bp: 40–60 °C), a red solid was obtained (444.9 mg, 0.68 mmol).

Alternative synthetic method: [$Pd(CH_3)Cl$(cod)] (119.9 mg, 0.45 mmol) was kept in a Schlenk flask and dissolved in CH_2Cl_2 (1.5 mL). A solution of the crude oil (containing 1.1 equiv of **1**; for exact quantities of **1** in the oil, see later) in CH_2Cl_2 (3 mL) was added. The reaction mixture was protected from light, stirred at RT for 45 min, and then concentrated at half volume under vacuum. Upon addition of petroleum ether (bp: 40–60 °C), a red solid was obtained (242.6 mg, 0.37 mmol).

Quantification of **1** in the crude oil: In addition to **1**, 2,6-dimethyl aniline (*ortho*) and 3,5-bis(trifluoromethyl) aniline (*meta*) were present in the crude oil. The following system of equations [Eqs. (1)–(3)] was used to quantify the amount of these compounds in the mixture:

$$\text{Oil weight} = n_{ortho}(FW_{ortho}) + n_{meta}(FW_{meta}) + n_1(FW_1) \quad (1)$$

$$n_{ortho} = an_1 \quad (2)$$

$$n_{meta} = bn_1 \quad (3)$$

For which *a* and *b* are the ratios between the integrals of both aniline peaks and the integrals of the **1** peak divided by the correct amount of protons. The following peaks in the ^{1}H NMR spectrum of the crude oil recorded in CD_2Cl_2 were chosen for the integration: 7.06 (3,5-bis(trifluoromethyl) aniline), 2.15 (2,6-dimethyl aniline), and 2.10 ppm (**1**).

[$Pd(CH_3)Cl$(1)] (1 a)

Yield: 89.5%. MS (ESI): *m/z* (%): 654.0 $[M+H]^+$; found: C 53.82, H 3.41, N 4.41; elemental analysis calcd (%) for $PdC_{29}H_{21}N_2ClF_6$: C 53.31, H 3.24, N 4.29; isomeric ratio *trans*/*cis*: CD_2Cl_2, 298 K: 1/19.

^{1}H NMR (500 MHz, CD_2Cl_2, 298 K): Major isomer (*trans*): $\delta = 8.16$ (dd, $^3J = 8.3$, 2H; $H^{5,8}$), 7.98 (s, 3H; $H^{14,16,18}$), 7.57 (t, $^3J = 7.8$, 1H; H^4), 7.49 (t, $^3J = 7.8$, 1H; H^9), 7.39–7.29 (m, 3H; $H^{15',16',17'}$), 7.22 (d, $^3J = 7.3$, 1H; H^3), 6.57 (d, $^3J = 7.3$, 1H; H^{10}), 2.30 (s, 6H; Ar–CH_3), 0.72 ppm (s, 3H; Pd–CH_3). Minor isomer (*cis*): $\delta = 8.08$ (s, 1H; H^{16}), 7.88 (s, 2H; $H^{14,18}$), 7.26 (m, 3H; $H^{15',16',17'}$), 6.79 (d, $J = 7.8$, 1H; H^{10}), 6.65 (d, $J = 7.8$, 1H; H^3), 2.33 (s, 6H; Ar–CH_3), 0.68 ppm (s, 3H; Pd–CH_3).

^{13}C NMR (126 MHz, CD_2Cl_2, 298 K): Major isomer (*trans*): $\delta = 132.2$ (C^5 or C^8), 132.0 (C^5 or C^8), 129.7 (C^9), 129.3 ($C^{16'}$), 128.9 (C^4), 127.9 ($C^{15',17'}$), 124.9 (C^3), 124.7 (C^{10}), 123.5 (C^{16}), 121.4 ($C^{14,18}$), 18.2 (Ar–CH_3), 1.8 ppm (Pd–CH_3).

Synthesis of [$Pd(CH_3)(NCCH_3)$(1)][PF_6] (1 b)

A solution of $AgPF_6$ (101.5 mg, 0.401 mmol) in CH_3CN (1 mL) was added to a solution of complex **1 a** (228.2 mg, 0.349 mmol) in CH_2Cl_2 (2 mL). The solution was stirred at RT for 30 min, and AgCl was filtered over celite; the solution was then concentrated at half volume under vacuum. Upon addition of diethyl ether, the product precipitated as a yellow solid (249.6 mg, 0.310 mmol).

[$Pd(CH_3)(NCCH_3)$(1)][PF_6] (1 b)

Yield: 88.8%; found: C 46.77, H 3.24, N 5.19; elemental analysis calcd (%) for $PdC_{31}H_{24}N_3PF_{12}$: C 46.32, H 3.01, N 5.23; isomeric ratio *trans*/*cis*: CD_2Cl_2, 298 K: 1/10.

^{1}H NMR (500 MHz, CD_2Cl_2, 298 K): Major isomer (*trans*): $\delta = 8.27$ (d, $J = 8.8$, 2H; H^5), 8.25 (d, $J = 8.8$, 2H; H^8), 8.11 (s, 1H; H^{16}), 8.04 (s, 2H; $H^{14,18}$), 7.66 (t, $J = 7.9$, 1H; H^4), 7.57 (t, $J = 7.9$, 1H; H^9), 7.41 (m, 1H; $H^{16'}$), 7.38–7.31 (m, 3H; $H^{14',18',3}$), 6.56 (d, $J = 7.3$, 1H; H^{10}), 2.28 (s, 6H; Ar–CH_3), 2.19 (s, 3H; Pd–$NCCH_3$), 0.85 ppm (s, 3H; Pd–CH_3). Minor isomer (*cis*): 8.15 (s, 1H; H^{16}), 7.89 (s, 2H; $H^{14,18}$), 7.01 (d, $J = 7.2$, 1H; H^{10}), 6.66 (d, $J = 7.6$, 1H; H^3), 2.39 (s, 6H; Ar–CH_3), 0.79 ppm (s, 3H, Pd–CH_3).

^{13}C NMR (126 MHz, CD_2Cl_2, 298 K): Major isomer (*trans*): $\delta = 133.8$ (C^5), 133.6 (C^8), 130.2 (C^9), 129.7 ($C^{14',18'}$), 129.6 (C^4), 125.8 (C^3), 125.7 (C^{10}), 122.7 ($C^{14,18}$), 122.5 (C^{16}), 18.0 (Ar–CH_3), 3.1 (Pd–NCCH_3), 7.8 ppm (Pd–CH_3).

IR (Nujol): $\tilde{\nu} = 846$ (s), 559 cm^{-1} (s) (PF_6^-).

Synthesis of dmso derivatives [Pd(CH_3)(dmso)(Ar-BIAN)][PF_6] (1c, 2c, 4c)

$AgPF_6$ (0.132 mmol) was added as a solid to a solution of the neutral complex (0.115 mmol) in CH_2Cl_2 (2 mL) containing dmso (0.132 mmol). The solution was stirred at RT for 30 min, and AgCl was filtered over Celite; the solution was then concentrated at half volume under vacuum. Upon addition of diethyl ether, the product precipitated as a yellow solid (average yield: 62.0%).

[Pd(CH_3)(dmso)(1)][PF_6] (1c)

Yield: 58.3%; found: C 44.16, H 3.18, N 2.28; elemental analysis calcd (%) for $PdC_{31}H_{27}N_2PF_{12}SO$: C 44.27, H 3.24, N 3.33; isomeric ratio (*cis*, dmso-S)/(*trans*, dmso-O)/(*trans*, dmso-S): CD_2Cl_2, 233 K: 2/3/13.

^{1}H NMR (500 MHz, CD_2Cl_2, 233 K): Major isomer (*trans*, dmso-S): $\delta =$ 8.26 (d, $^3J = 8.3$, 2H; $H^{5,8}$), 8.04 (s, 1H; H^{16}), 7.92 (s, 2H; $H^{14,18}$), 7.61–7.53 (m, 2H; $H^{4,9}$), 7.40 (dd, $J = 8.3$, 6.8, 1H; $H^{16'}$), 7.34 (d, $J = 7.5$, 2H; $H^{15',17'}$), 6.73 (d, $J = 7.4$, 1H; H^3), 6.54 (d, $J = 7.3$, 1H; H^{10}), 3.07 (s, 6H; $(CH_3)_2SO$), 2.24 (s, 6H; Ar–CH_3), 0.51 ppm (s, 3H; Pd–CH_3). Minor isomer (*cis*, dmso-S): $\delta = 8.21$–8.18 (m, 2H; $H^{5,8}$), 8.16 (s, 1H; H^{16}), 7.95 (s, 2H; $H^{14,18}$), 6.64 (d, $J = 7.4$, 1H; H^{10}), 6.58 (d, $J = 7.4$, 1H; H^3), 2.88 (s, 6H; $(CH_3)_2SO$), 2.29 (s, 6H; Ar–CH_3), 0.73 ppm (s, 3H; Pd–CH_3). Minor isomer (*trans*, dmso-O): $\delta = 8.26$ (d, $J = 8.3$, 1H; H^5), 8.21–8.18 (m, 1H; H^8), 7.99 (s, 1H; H^{16}), 7.79 (s, 2H; $H^{15,17}$), 7.53–7.48 (m, 1H; H^9), 7.16 (d, $J = 7.3$, 1H; H^3), 6.48 (d, $J = 7.5$, 1H; H^{10}), 2.86 (s, 6H; $(CH_3)_2SO$), 2.20 (s, 6H; Ar–CH_3), 0.84 ppm (s, 3H; Pd–CH_3).

^{1}H NMR (500 MHz, [D_6]DMSO, 298 K): $\delta = 8.40$ (d, $J = 8.3$, 1H; $H^{5\text{ or }8}$), 8.37 (d, $J = 8.3$, 1H; $H^{5\text{ or }8}$), 8.32 (s, 2H; $H^{14,18}$), 8.28 (s, 1H; H^{16}), 7.78–7.66 (m, 2H; $H^{4,9}$), 7.41 (s, 3H; $H^{15',16',17'}$), 6.71 (d, $J = 7.1$, 1H; $H^{3\text{ or }10}$), 6.48 (d, $J = 7.1$, 1H; $H^{3\text{ or}10}$), 2.29 (s, 6H; Ar–CH_3), 0.52 ppm (s, 3H; Pd–CH_3).

^{13}C NMR (126 MHz, CD_2Cl_2, 233 K): Major isomer (*trans*, dmso-S): $\delta =$ 133.5 (C^5 or C^8), 133.4 (C^5 or C^8), 121.7 (C^{16}), 122.2 ($C^{14,18}$), 129.0 (C^4), 129.5 (C^9), 128.6 ($C^{16'}$), 129.3 ($C^{15',17'}$), 126.3 (C^3), 126.0 (C^{10}), 45.1 ($(CH_3)_2SO$), 18.1 ppm (Ar–CH_3), 10.9 (Pd–CH_3). Minor isomer (*cis*, dmso-S): $\delta = 122.5$ (C^{16}), 122.7 ($C^{14,18}$), 125.8 (C^{10}), 126.4 (C^3), 44.5 ($(CH_3)_2SO$), 18.1 (Ar–CH_3), 15.2 ppm (Pd–CH_3). Minor isomer (*cis*, dmso-O): $\delta = 134.2$ (C^5), 121.6 (C^{16}), 122.6 ($C^{14,18}$), 129.6 (C^9), 125.0 (C^3), 125.1 (C^{10}), 37.5 ($(CH_3)_2SO$), 17.9 (Ar–CH_3), 7.6 ppm (Pd–CH_3).

^{13}C NMR (126 MHz, [D_6]DMSO, 298 K): $\delta = 133.1$ ($C^{5\text{ or }8}$), 132.3 ($C^{5\text{ or }8}$), 123.2 ($C^{14,18}$), 121.1 (C^{16}), 129.4 ($C^{4,9}$), 128.8 ($C^{15',16',17'}$), 125.2 ($C^{3\text{ or }10}$), 124.3 ($C^{3\text{ or }10}$), 17.6 (Ar–CH_3), 9.4 ppm (Pd–CH_3).

IR (Nujol): $\tilde{\nu} = 1139$ (s) and 975 (m) (S=O), 847 (s) and 558 cm^{-1} (s) (PF_6^-).

[Pd(CH_3)(dmso-S)(2)][PF_6] (2c)

Yield: 62.3%; found: C 50.76, H 4.48, N 3.84; elemental analysis calcd (%) for $PdC_{31}H_{33}N_2PF_6SO$: C 50.79, H 4.54, N 3.82.

^{1}H NMR (500 MHz, CD_2Cl_2, 298 K): $\delta = 8.23$ (d, $J = 8.3$, 1H; $H^{5\text{ or }8}$), 8.20 (d, $J = 8.3$, 1H; $H^{5\text{ or }8}$), 7.57 (t, $J = 7.8$, 2H; $H^{4,9}$), 7.47–7.42 (m, 1H; Ar–H), 7.41–7.36 (m, 3H; Ar–H), 7.36–7.32 (m, 2H; Ar–H), 6.71 (d, $J = 7.3$, 1H; H^3), 6.61 (d, $J = 7.3$, 1H; H^{10}), 2.89 (s, 6H; $(CH_3)_2SO$), 2.34 (s, 6H; Ar–CH_3), 2.29 (s, 6H; Ar–CH_3), 0.83 ppm (s, 3H; Pd–CH_3).

^{13}C NMR (126 MHz, CD_2Cl_2, 298 K): $\delta = 134.1$ ($C^{5\text{ or }8}$), 133.3 ($C^{5\text{ or }8}$), 130.0 ($C^{4,9}$), 129.3 (C^{Ar}), 129.7 (C^{Ar}), 129.8 (C^{Ar}), 126.0 (C^3), 126.3 (C^{10}), 45.1 ($(CH_3)_2SO$), 18.2 (Ar–CH_3), 14.6 ppm (Pd–CH_3).

IR (Nujol): $\tilde{\nu} = 1123$ cm^{-1} (S=O), 868 (s) and 556 cm^{-1} (s) (PF_6^-).

[Pd(CH_3)(dmso)(4)][PF_6] (4c)

Yield: 65.5%; found: C 39.04, H 2.20, N 2.93; elemental analysis calcd (%) for $PdC_{31}H_{21}N_2PF_{18}SO$: C 39.24, H 2.23, N 2.95; isomeric ratio (dmso-O)/(dmso-S): CD_2Cl_2, 223 K: 2/3.

^{1}H NMR (500 MHz, CD_2Cl_2, 223 K): Major isomer (dmso-S): $\delta = 8.33$–8.17 (m, 2H; $H^{5,8}$), 7.90 (s, 5H; $H^{14,18,14',18'}$ and $H^{16\text{ or }16'}$), 7.79 (s, 1H; $H^{16\text{ or }16'}$), 7.64–7.50 (m, 2H; $H^{4,9}$), 7.23–7.15 (m, 1H; H^3), 6.67–6.46 (m, 1H; H^{10}), 3.04 (s, 6H; $(CH_3)_2SO$), 0.48 ppm (s, 3H; Pd–CH_3). Minor isomer (dmso-O): $\delta = 8.33$–8.17 (m, 2H; $H^{5,8}$), 8.17–7.96 (m, 5H; $H^{14,18,14',18'}$ and $H^{16\text{ or }16'}$), 7.93 (m, 1H; $H^{16\text{ or }16'}$), 7.64–7.50 (m, 2H; $H^{4,9}$), 7.23–7.15 (m, 1H; H^3), 6.67–6.46 (m, 1H; H^{10}), 2.71 (s, 6H; $(CH_3)_2SO$), 0.67 ppm (s, 3H; Pd–CH_3).

^{13}C NMR (126 MHz, CD_2Cl_2, 223 K). Major isomer (dmso-S): $\delta = 132.8$ ($C^{5\text{ or }8}$), 132.3 ($C^{5\text{ or }8}$), 129.1 ($C^{4,9}$), 125.3 (C^{10}), 125.1 (C^3), 122.4 ($C^{16,16'}$), 122.2 ($C^{14,18,14',18'}$), 45.2 ($(CH_3)_2SO$), 11.23 ppm (Pd–CH_3). Minor isomer (dmso-O): $\delta = 126.5$ (C^{10}), 122.0 ($C^{14,18,14',18'}$), 121.4 ($C^{16,16'}$), 38.83 ($(CH_3)_2SO$), 3.05 ppm (Pd–CH_3).

IR (Nujol): $\tilde{\nu} = 1131$ (s) and 984 cm^{-1} (m) (S=O), 868 (s) and 556 cm^{-1} (s) (PF_6^-).

Cooligomerization reactions

All catalytic experiments were performed in a Büchi tinyclave glass reactor equipped with an interchangeable 50 mL glass vessel. The vessel was loaded with the desired complex (21 μmol), 2,2,2-trifluoroethanol (21 mL), and MA (1.13 mL). The reactor was then placed in a preheated oil bath, connected to the ethylene tank, and pressurized. The reaction mixture was stirred at constant temperature and pressure. After the appropriate time, the reactor was cooled to RT and vented. An aliquot (200 μL) of the reaction mixture was withdrawn and diluted in CH_3OH (1 mL) for GC–MS analyses. The reaction mixture was poured in a 50 mL round flask, together with dichloromethane (3×2 mL) used to wash the glass vessel. No separation of palladium black was performed. Volatiles were removed under reduced pressure, and the residual oil was dried at constant weight and analyzed by using ^{1}H NMR spectroscopy.

Ethylene/MA cooligomer

^{1}H NMR (500 MHz, $CDCl_3$, 298 K): $\delta = 5.57$–4.90 (m; CH=CH), 3.60 (s; OCH_3), 2.24 (t, $J = 7.5$; $CH_2C(O)$), 2.09–1.79 (m; CH_2CH=CH), 1.68–1.46 (m; $CH_2CH_2C(O)$, CH_3CH=CH), 1.46–0.99 (m; –(CH_2)–, –CH(*R*)–), 0.99–0.86 (m; CH_3CH_2CH=CH, –CH_3), 0.86–0.63 ppm (m, –CH_3).

^{13}C NMR (126 MHz, $CDCl_3$, 223 K): Characteristic resonances due to the functionalized cooligomer: $\delta = 173.9$ (C(O)), 51.1 (OCH_3), 33.9 ($CH_2C(O)$), 24.8 ppm ($CH_2CH_2C(O)$).

In situ NMR investigations

A 10 mM CD_2Cl_2 solution of the complex in the NMR tube was reacted with the monomer (see later) kept in the spectrometer at 298 K, and the Varian pad experiment was performed on it, with time delay set to 300 s. The required time for each ^1H NMR experiment (60 s) was taken into account when analyzing the kinetic data.

Ethylene: In the case of the apolar monomer, the NMR tube was kept in a suitable Schlenk flask and ethylene was bubbled through a cannula coaxial to the tube and connected to the ethylene tank. The tip of the cannula was kept 2 cm above the interphase to avoid any loss of solution.

Methyl acrylate: In the case of the polar monomer, MA (2 equiv) was added to the solution through a 10 μL syringe.

Detected intermediates

^1H NMR (500 MHz, CD_2Cl_2, 298 K): **1b(C")**: $\delta = 8.25$ (m, 2H; $H^{5,8}$), 8.06 (s, 1H; H^{16}), 8.04 (s, 2H; $H^{14,18}$), 7.64 (t, $J = 7.8$, 1H; H^4), 7.55 (t, $J = 7.8$, 1H; H^9), 7.44–7.38 (m, 1H; $H^{16'}$), 7.38–7.33 (m, 2H; $H^{14',18'}$), 7.24 (d, $J = 7.3$, 1H; H^3), 6.56 (d, $J = 7.3$, 1H; H^{10}), 3.42 (s, 3H; OCH_3), 2.64–2.56 (m, 2H; $CH_2C(O)$), 2.32 (s, 6H; Ar–CH_3), 1.71 (t, $J = 5.9$, 2H; Pd–$CH_2CH_2CH_2C(O)$), 0.74 ppm (pentet, $J = 5.9$, 2H; $CH_2CH_2C(O)$); **1b(B")**: $\delta = 1.81$ (m, 1H; Pd–$CH(CH_3)$), 0.43 ppm (d, $J = 7.1$, 3H; Pd–$CH(CH_3)$); **1b(A')**: $\delta = 2.33$ (m, 1H; $CH(CH_3)$), 0.69 (m, 3H; $CH(CH_3)$); **1b(D')**: $\delta = 3.75$ (s, 3H; OCH_3), 2.49 (t, $J = 6.9$, 1H; $CH_2C(O)$), 1.65 ppm (t, $J = 6.9$, 1H; Pd–CH_2).

^{13}C NMR (126 MHz, CD_2Cl_2, 298 K): **1b(C")**: $\delta = 183.5$ (C(O)), 133.4 ($C^{5,8}$), 130.0 (C^9), 129.8 ($C^{14',18'}$), 129.3 (C^4), 129.0 ($C^{16'}$), 125.8 (C^3), 125.6 (C^{10}), 122.5 ($C^{14,18}$), 122.1 (C^{16}), 54.9 (OCH_3), 36.1 ($CH_2C(O)$), 31.7 ($PdCH_2CH_2CH_2C(O)$), 24.0 ($CH_2CH_2C(O)$), 18.0 ppm (Ar–CH_3); **1b(B")**: $\delta = 34.7$ (Pd–$CH(CH_3)$), 21.9 ppm (Pd–$CH(CH_3)$); **1b(A')**: $\delta = 36.5$ ($CH(CH_3)$), 17.7 ($CH(CH_3)$); **1b(D')**: $\delta = 191.3$ (C(O)), 55.5 ($C(O)OCH_3$), 37.9 ppm ($CH_2C(O)$).

Acknowledgements

This work was financially supported by the Italian MIUR (PRIN N° 207HMTJWP 002). Fondazione CRTrieste and Fondazione Benefica Kathleen Foreman Casali are gratefully acknowledged for the generous donations of a Varian 500 MHz spectrometer and a Büchi tinyclave glass reactor, respectively. P.F. and T.M. acknowledge Consorzio Interuniversitario Nazionale per la Scienza e Tecnologia dei Materiali for financial support.

Keywords: ethylene · N ligands · oligomerization · palladium · polar monomer

[1] A. Nakamura, S. Ito, K. Nozaki, *Chem. Rev.* **2009**, *109*, 5215 – 5244.
[2] A. Berkefeld, S. Mecking, *Angew. Chem.* **2008**, *120*, 2572 – 2576; *Angew. Chem. Int. Ed.* **2008**, *47*, 2538 – 2542.
[3] A. Sen, S. Borkar, *J. Organomet. Chem.* **2007**, *692*, 3291 – 3299.
[4] J.-Y. Dong, Y. Hu, *Coord. Chem. Rev.* **2006**, *250*, 47 – 65.
[5] L. S. Boffa, B. M. Novak, *Chem. Rev.* **2000**, *100*, 1479 – 1494.
[6] S. Ito, K. Nozaki, *Chem. Rec.* **2010**, *10*, 315 – 325.
[7] J. A. Gladysz, Z. T. Ball, G. Bertrand, S. A. Blum, V. M. Dong, R. Dorta, F. E. Hahn, M. G. Humphrey, W. D. Jones, J. Klosin, I. Manners, T. J. Marks, J. M. Mayer, B. Rieger, J. C. Ritter, A. P. Sattelberger, J. M. Schomaker, V. W.-W. Yam, *Organometallics* **2012**, *31*, 1 – 18.
[8] L. K. Johnson, C. M. Killian, M. Brookhart, *J. Am. Chem. Soc.* **1995**, *117*, 6414 – 6415.
[9] S. D. Ittel, L. K. Johnson, M. Brookhart, *Chem. Rev.* **2000**, *100*, 1169 – 1204.
[10] L. K. Johnson, S. Mecking, M. Brookhart, *J. Am. Chem. Soc.* **1996**, *118*, 267 – 268.
[11] S. Mecking, L. K. Johnson, L. Wang, M. Brookhart, *J. Am. Chem. Soc.* **1998**, *120*, 888 – 899.
[12] E. Drent, R. van Dijk, R. van Ginkel, B. van Oort, R. I. Pugh, *Chem. Commun.* **2002**, 744 – 745.
[13] T. Kochi, K. Yoshimura, K. Nozaki, *Dalton Trans.* **2006**, 25 – 27.
[14] D. Guironnet, P. Roesle, T. Runzi, I. Gottker-Schnetmann, S. Mecking, *J. Am. Chem. Soc.* **2009**, *131*, 422 – 423.
[15] S. Ito, K. Munakata, A. Nakamura, K. Nozaki, *J. Am. Chem. Soc.* **2009**, *131*, 14606 – 14607.
[16] T. Kochi, S. Noda, K. Yoshimura, K. Nozaki, *J. Am. Chem. Soc.* **2007**, *129*, 8948 – 8949.
[17] S. Ito, M. Kanazawa, K. Munakata, J. Kuroda, Y. Okumura, K. Nozaki, *J. Am. Chem. Soc.* **2011**, *133*, 1232 – 1235.
[18] S. Luo, J. Vela, G. R. Lief, R. F. Jordan, *J. Am. Chem. Soc.* **2007**, *129*, 8946 – 8947.
[19] W. Weng, Z. Shen, R. F. Jordan, *J. Am. Chem. Soc.* **2007**, *129*, 15450 – 15451.
[20] K. M. Skupov, J. Hobbs, P. Marella, D. Conner, S. Golisz, B. L. Goodall, J. P. Claverie, *Macromolecules* **2009**, *42*, 6953 – 6963.
[21] K. M. Skupov, L. Piche, J. P. Claverie, *Macromolecules* **2008**, *41*, 2309 – 2310.
[22] C. S. Popeney, D. H. Camacho, Z. Guan, *J. Am. Chem. Soc.* **2007**, *129*, 10062 – 10063.
[23] S. Luo, R. F. Jordan, *J. Am. Chem. Soc.* **2006**, *128*, 12072 – 12073.
[24] X. B. Shi, Y. Zhao, H. Y. Gao, L. Zhang, F. M. Zhu, Q. Wu, *Macromol. Rapid Commun.* **2012**, *33*, 374 – 379.
[25] B. P. Carrow, K. Nozaki, *J. Am. Chem. Soc.* **2012**, *134*, 8802 – 8805.
[26] A. Scarel, M. R. Axet, F. Amoroso, F. Ragaini, C. J. Elsevier, A. Holuigue, C. Carfagna, L. Mosca, B. Milani, *Organometallics* **2008**, *27*, 1486 – 1494.
[27] T. Rünzi, D. Guironnet, I. Göttker-Schnetmann, S. Mecking, *J. Am. Chem. Soc.* **2010**, *132*, 16623 – 16630.
[28] B. Neuwald, F. Ölscher, I. Göttker-Schnetmann, S. Mecking, *Organometallics* **2012**, *31*, 3128 – 3137.
[29] M. Gasperini, F. Ragaini, E. Gazzola, A. Caselli, P. Macchi, *Dalton Trans.* **2004**, 3376 – 3382.
[30] R. van Asselt, C. J. Elsevier, W. J. J. Smeets, A. L. Spek, R. Benedix, *Recl. Trav. Chim. Pays-Bas* **1994**, *113*, 88 – 98.
[31] N. J. Hill, I. Vargas-Baca, A. H. Cowley, *Dalton Trans.* **2009**, 240 – 253.
[32] J. Kovach, M. Peralta, W. W. Brennessel, W. D. Jones, *J. Mol. Struct.* **2011**, *992*, 33 – 38.
[33] U. El-Ayaan, F. Murata, S. El-Derby, Y. Fukuda, *J. Mol. Struct.* **2004**, *692*, 209 – 216.
[34] D. N. Coventry, A. S. Batsanov, A. E. Goeta, J. A. K. Howard, T. B. Marder, *Polyhedron* **2004**, *23*, 2789 – 2795.
[35] I. L. Fedushkin, V. A. Chudakova, A. A. Skatova, N. M. Khvoinova, Y. A. Kurskii, T. A. Glukhova, G. K. Fukin, S. Dechert, M. Hummert, H. Schumann, *Z. Anorg. Allg. Chem.* **2004**, *630*, 501 – 507.
[36] V. Rosa, T. Aviles, G. Aullon, B. Covelo, C. Lodeiro, *Inorg. Chem.* **2008**, *47*, 7734 – 7744.
[37] R. van Asselt, E. E. C. G. Gielens, R. E. Rulke, C. J. Elsevier, *J. Chem. Soc. Chem. Commun.* **1993**, 1203 – 1205.
[38] R. E. Rülke, J. M. Ernsting, A. L. Spek, C. J. Elsevier, P. W. N. M. Van Leeuwen, K. Vrieze, *Inorg. Chem.* **1993**, *32*, 5769 – 5778.
[39] V. Khlebnikov, A. Meduri, H. Mueller-Bunz, T. Montini, P. Fornasiero, E. Zangrando, B. Milani, M. Albrecht, *Organometallics* **2012**, *31*, 976 – 986.
[40] J. Zhou, H. Sun, K. Harms, J. Sundermeyer, *Z. Anorg. Allg. Chem.* **2008**, *634*, 1517 – 1521.
[41] J. Durand, E. Zangrando, M. Stener, G. Fronzoni, C. Carfagna, B. Binotti, P. C. J. Kamer, C. Muller, M. Caporali, P. W. N. M. van Leeuwen, D. Vogt, B. Milani, *Chem. Eur. J.* **2006**, *12*, 7639 – 7651.
[42] J. D. Fotheringham, G. A. Heath, A. J. Lindsay, T. A. Stephenson, *J. Chem. Res. (S)* **1986**, 82 – 83.
[43] A. Bastero, A. Ruiz, C. Claver, B. Milani, E. Zangrando, *Organometallics* **2002**, *21*, 5820 – 5829.

[44] A. Bastero, C. Claver, A. Ruiz, S. Castillon, E. Daura, C. Bo, E. Zangrando, *Chem. Eur. J.* **2004**, *10*, 3747 – 3760.
[45] A. Scarel, J. Durand, D. Franchi, E. Zangrando, G. Mestroni, B. Milani, S. Gladiali, C. Carfagna, B. Binotti, S. Bronco, T. Gragnoli, *J. Organomet. Chem.* **2005**, *690*, 2106 – 2120.
[46] M. R. Axet, F. Amoroso, G. Bottari, A. D'Amora, E. Zangrando, F. Faraone, D. Drommi, M. Saporita, C. Carfagna, P. Natanti, R. Seraglia, B. Milani, *Organometallics* **2009**, *28*, 4464 – 4474.
[47] A. D'Amora, L. Fanfoni, D. Cozzula, N. Guidolin, E. Zangrando, F. Felluga, S. Gladiali, F. Benedetti, B. Milani, *Organometallics* **2010**, *29*, 4472 – 4485.
[48] D. J. Tempel, L. K. Johnson, R. L. Huff, P. S. White, M. Brookhart, *J. Am. Chem. Soc.* **2000**, *122*, 6686 – 6700.
[49] E. F. McCord, S. J. McLain, L. T. J. Nelson, S. D. Ittel, D. Tempel, C. M. Killian, L. K. Johnson, M. Brookhart, *Macromolecules* **2007**, *40*, 410 – 420.
[50] E. F. McCord, S. J. McLain, L. T. J. Nelson, S. D. Arthur, E. B. Coughlin, S. D. Ittel, L. K. Johnson, D. Tempel, C. M. Killian, M. Brookhart, *Macromolecules* **2001**, *34*, 362 – 371.
[51] T. Usami, S. Takayama, *Macromolecules* **1984**, *17*, 1756 – 1761.
[52] D. E. Axelson, G. C. Levy, L. Mandelkern, *Macromolecules* **1979**, *12*, 41 – 52.
[53] P. Braunstein, C. Frison, X. Morise, *Angew. Chem.* **2000**, *112*, 2989 – 2992; *Angew. Chem. Int. Ed.* **2000**, *39*, 2867 – 2870.
[54] M. Agostinho, P. Braunstein, *Chem. Commun.* **2007**, 58 – 60.
[55] S. Borkar, H. Yennawar, A. Sen, *Organometallics* **2007**, *26*, 4711 – 4714.
[56] E. Zuidema, C. Bo, P. W. N. M. van Leeuwen, *J. Am. Chem. Soc.* **2007**, *129*, 3989 – 4000.
[57] M. Gasperini, F. Ragaini, S. Cenini, *Organometallics* **2002**, *21*, 2950 – 2957.

Received: July 31, 2012
Published online on November 5, 2012